Plasmonics
DOI 10.1007/s11468-013-9540-z

Effects of Refractive Index Variations on the Optical Transmittance Spectral Properties of the Nano-Hole Arrays

Mehrdad Irannejad · Bo Cui

Received: 20 November 2012 / Accepted: 4 March 2013

Abstract The 3D finite difference time domain technique was carried out to study the optical transmission properties of nano-hole arrays in the gold thin film supported by materials with different index of refraction in the visible and infrared regions. A series of perforated nano-hole structures on the gold film at different hole radius, hole depth of 100 nm, and structural periodicity of 400 nm were studied. It was found that transmission properties (i.e., intensity, FWHM, and resonance position) were strongly affected by hole radius and surrounding medium index of refraction. The maximum optical transmittance was observed as 31.9 % in a nano-hole array of hole radius of 125 nm and refractive index of 1.3. The maximum sensitivity of 300 nm/RIU was obtained at index of refraction of 1.7, whereas the minimum one was calculated as 110 nm/RIU in a nano-hole array of hole radius of 50 nm. It was also found that on increasing the hole radius from 50 to 125 nm, the spectral sensitivity was decreased, whereas the index sensitivity was increased on increasing the refractive index.

Keywords FDTD · EOT · Optical transmission · Nano-hole · Plasmonic

Introduction

Optical transmission and its properties through nano-hole arrays (NHAs) have been studied well for a decade, and many theoretical and experimental works developed back to 1998, where the discovery by Ebbesen et al. of extraordinary optical transmission (EOT) [1] through NHA in the silver thin films, challenged the Bethe theory for diffraction of light through a small hole [2]. Although the Bethe theory predicts very small optical transmission through nano-holes in thin metallic film which is proportional to $(r/\lambda)^4$, an enhanced transmission up to 4 % was observed by Ebbesen [1]. Since the discovery of EOT, optical transmission enhancement through NHAs in metallic films involves many research groups in the world, and different configurations [3, 4] have been studied theoretically and experimentally to demonstrate transmission enhancement, EOT, and their applications.

M. Irannejad (✉) · B. Cui
Waterloo Institute for Nanotechnology, University of Waterloo, Waterloo, ON, Canada
e-mail: pm07mi@gmail.com

Surface plasmons (SPs) are collective oscillations of metal-free electrons trapped at metal–dielectric interfaces that are excited by incident electromagnetic field and confined in the metal surface. The coupling and decoupling phenomenon between the SP resonance evanescent waves and the incident light through the nano-hole lead to the multiple optical resonance peaks at higher transmission intensity when normalized to the aperture area [1]. Hence, SP resonance excitation, which could be controlled by adjusting the geometrical parameters, plays a crucial role to explain the observation of EOT [1, 5–7]. Refractive index of the substrate material and the hole medium, hole shape, hole radius, and structural periodicity are the main parameters that affect the resonance wavelength and its intensity [8–10]. Therefore, the EOT could be used as an active element by considering a minimum periodicity and minimum wavelength at metal–dielectric interface [1] to study the physical and chemical properties of different materials by monitoring the variation of refractive index [6, 11, 12]. Thus, enhanced transmission has potential application in many different areas such as bio- and chemical sensing [13], integrated nano- and micro-photonic, nano-photonics device (laser and waveguides) [14], microscopy and display technology, plasmonic photolithography [15, 16], and fluorescence microscopy [17, 18].

Published online: 15 March 2013

The transmission wavelength position and its intensity can precisely be controlled by nano-hole shape and nano-holes periodicity [13]. For example, in a short range structures with small number of holes, the contribution from the structural edges becomes more significant, leading to unusual emission patterns. Whilst the position of the resonance wavelength can be adjusted by variation of the periodicity independent of metal, film thickness and hole diameter [1], however, more tunability can be achieved by applying a magnetic field [19]. In periodic grating plasmonic materials, Rayleigh anomalies (RAs) and surface plasmon resonances (SPRs) from both side of films can be interfered under certain conditions and create highly narrow spectral features which can be described by Fano resonance and Fano lineshape models [20, 21]. In this paper, we report the theoretical study of optical transmission spectra of perforated NHA structure with different geometrical parameters and structures in the visible and infrared regions.

Analytical Theory and FDTD Simulation

In this work, a series of perforated circular NHA structures in gold thin film supported by substrate at different index of refraction (Fig. 1) and hole radiuses at fix hole depth of 100 nm and structural periodicity of 400 nm were studied. The effects of varying of hole radius and supported layer refractive index on the energy matching and transmittance properties of the incident light through the nano-holes square arrays were analyzed by using 3D finite difference time domain (FDTD) method, which is a reliable method in solving Maxwell's equations in dispersive media like gold and silver.

In Cartesian coordinate x, y, and z, a designated structure consists of a cladding air layer, a gold film supported by glass layer (Fig. 1). An air cylindrical nano-hole of radius, r, was considered in the gold film. Each medium was specified by relative permittivity, $\varepsilon(\omega)$. For substrate layer, $\varepsilon(\omega)$ was assumed as n^2 and the Lorentz–Drude model was employed to describe the permittivity of gold layer [22, 23]:

$$\varepsilon(\omega) = \varepsilon_\infty + \sum_{0}^{M} \frac{f_m \omega_P^2}{\omega_m - \omega^2 + i\omega\Gamma_m} \qquad (1)$$

where ε_∞ is the permittivity in the infinity frequency, ω and $\omega_p(= 1.37188 \times 10^{16}\ \mathrm{rad/s})$ are the incident and gold plasma frequencies, respectively, ω_m is the mth resonance frequency, and Γ_m is the mth damping frequency which is obtained by fitting the empirical data for real and imaginary parts of gold permittivity over a given wavelength range of interest [23; http://www.optiwave.com/products/gallery/optifdtd/fdtd%20files/OptiFDTD_10_Technical_Background_and_Tutorials.pdf].

The FDTD was carried out by using the OptiFDTD from Optiwave Inc. The periodic boundary condition in the x- and y-directions and anisotropic perfect matching layer in the z-direction was used as absorbing boundary condition to study the optical transmittance properties at normal incident of electromagnetic wave through the NHA perforated on the gold film which is supported by substrate layer of different refractive indices in the range of 1.0 to 1.7. In this study, a linearly polarized electromagnetic plane wave along y-axis (λ_{center}=680 nm, time offset=0.8×10^{-14}s, and half width=0.1×10^{-14}s) which propagates in the z-axis was assumed.

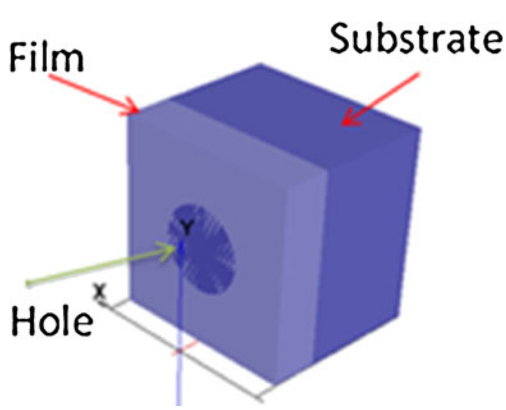

Fig. 1 A unit cell of a circular NHA perforated in the gold film supported by substrate layer

Result and Discussion

In general, for normal incident light, the maximum of the spectral resonance wavelength of transmission in a square NHA can approximately be calculated by the following equation [20, 24]:

$$\lambda_{SP}^{max}(i,j) = \frac{P}{\sqrt{i^2 + j^2}} \sqrt{\frac{\varepsilon_d \varepsilon_m}{\varepsilon_d + \varepsilon_m}} \qquad (2)$$

where P is the structural periodicity, ε_d and ε_m are the relative permittivity of the surrounded dielectric and metal, and i and j are integer numbers defining the different transmission diffraction orders. Therefore, there are two sets of resonance wavelengths associated with each surface, i.e., film/substrate and superstrate/film (i.e., air in this study) interfaces.

The effects of varying of hole radius and substrate refractive index on the optical transmission properties at normal incident through the circular NHAs will be discussed in the following sections.

Different Hole Radius

The optical transmittance spectrum of the gold-perforated circular NHAs of different hole radius in the range of

25–125 nm that were supported by silica substrate (n=1.5) is shown in Fig. 2a.

In this figure, the transmission resonance wavelengths in the range of 371 to 387 nm and 578 to 604 nm can be assigned to the $\lambda_{(1,\ 1)}$ and $\lambda_{(1,\ 0)}$ of the air/film interface, respectively. The surface plasmon resonance wavelength of $\lambda_{(1,\ 0)}$ of the film/substrate was observed in the range 690 to 743 nm, whereas the bulk plasmon resonance was acquired in the range of 476 to 481 nm in the NHA [25] as listed in Table 1. The difference between the NHA spectral resonance wavelengths and those that are calculated by Eq. 2 can be attributed to the interference between the surface plasmon resonance evanescent waves with the transmitted light through the nano-holes [25] and the negative phase shift due to SP scattering by air/nano-hole and nano-hole/substrate interfaces [3].

In Table 1, the phase shift in the NHA of different hole radiuses is also reported. As can be seen, the phase shift related to the $\lambda_{(1,\ 0)}$ was increased on increasing the hole radius, whereas the phase shift related to the $\lambda_{(1,\ 1)}$ was decreased.

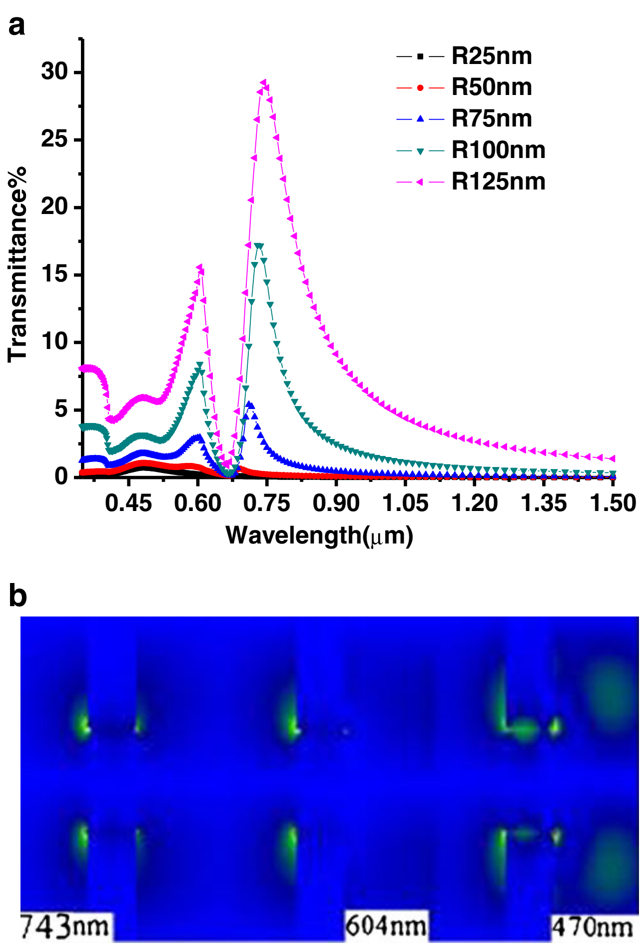

Fig. 2 **a** The transmittance spectrum at different hole radiuses and **b** the E_z filed distribution at different wavelength of a circular nano-hole array perforated in the gold film supported by silica at hole radius of 125, hole depth of 100 nm, and periodicity of 400 nm

A redshift was also observed in the film/substrate resonance peaks $\lambda_{(1,\ 0)}$ on increasing the hole radius as clear in Fig. 2a. Although, the bulk plasmon resonance was dominant resonance phenomena in the NHA of hole radius of 25 nm, there was no evidence of transmission resonances as it is evident from Fig. 2a. It is also clear that there is a distinct minimum and maximum at 664 and 743 nm. This might be due to the RAs and SPR interference and can be explained by Fano resonance which is an asymmetric interference between the SPR with the incident light inside the nano-holes [20, 21].

Figure 2b shows the electric field along z-axis of the NHA at a hole radius of 125 nm and substrate refractive index of 1.5 at different resonance wavelengths. As can be seen from this figure, the electric field at 743 nm is localized at both input (air/film) and output (film/substrate) interfaces; however, the electric field at 604 nm was only localized at the air/film interface. The bulk plasmon resonance was observed at 470 nm as photonic propagation mode.

The effects of varying of hole radius on the resonance wavelength position, full width at half maximum (FWHM), and transmission intensity of the $\lambda_{(1,\ 0)}$ resonance mode are shown in Fig. 3. As can be seen from this figure, the transmission intensity was increased linearly on increasing the hole radius. This could be attributed to the larger amount of transmitted light through the nano-hole and therefore stronger coupling between the SP resonance evanescent waves with the guided electromagnetic wave through the hole in both input and output interfaces.

The effects of varying of hole radius in a NHA structure on the FWHM value of the $\lambda_{(1,\ 0)}$ resonance mode were also shown in Fig. 3. It was found that the FWHM value was comparable for hole radiuses of 50 and 75 nm; however, it was linearly increased on increasing the hole radius beyond the 75 nm and its maximum was acquired as 122.5 nm for hole radius of 125 nm. The main reason of smaller FWHM values in the nano-hole structure with hole radiuses of 50 and 75 nm rather than larger radiuses can be attributed to the effects of the hole edges on the transmission spectrum and smaller amount of light that was coupled with the SP evanescent waves inside the hole structure [1, 13].

The effects of varying of hole radius on the resonance position of the first transmission diffraction order, $\lambda_{(1,\ 0)}$, are also shown in Fig. 3. From this figure, it is clear that on increasing the hole radius, the fundamental resonance position shifts towards longer wavelengths, and by increasing the hole radius of 100 nm, the resonance positions increased by 51 nm. It was also found that, on increasing the hole radius to 150 nm, the SPR transmission wavelength was shifted to 771 nm and then saturated for larger radiuses, which is in good agreement with that reported by Wu et.al [5].

Table 1 The surface plasmon resonance and phase shift of different transmission diffraction orders in a series of nano-hole array with different hole radius, hole depth of 100 nm, period of 400 nm, and substrate refractive index of 1.5

Hole_r (nm)	Bulk plasmon (nm)	Film/sub-interface	Air/film interface		Phase shift (rad)		
					Film/sub-interface	Air/film interface	
		1, 0	1, 0	1, 1	1, 0	1, 0	1, 1
50	484	690	578	387	−0.34	−0.217	−2.0
75	481	710	604	375	−0.41	−0.062	−1.90
100	476	729	604	371	−0.57	−0.062	−1.85
125	476	743	604	371	−0.68	−0.062	−1.85

Furthermore, optical transmittance with the maximum transmission of 26.2 % and strongest electric filed enhancement were acquired at a hole radius of 125 nm at wavelength of 743 nm which were exceeded several times larger than that predicted by Bethe's theory [2]. Whilst the minimum transmission of 0.478 % was obtained at a hole radius of 50 nm and wavelength of 690 nm in a NHA perforated in the gold film that was supported by silica, which indicates no SP-enhanced transmittance [26] was observed at hole radius of 50 nm on such NHA structure.

Different Substrate Index

The effects of varying of refractive index in the range of 1 to 1.7 of the supported material (i.e., substrate) on the optical transmittance spectra in NHA structure are compared in Fig. 4a. As can be seen from this figure, on increasing the substrate refractive index, the optical transmission shows a redshift of 185 nm in the resonance peak position of the first transmission diffracted order, $\lambda_{(1,\ 0)}$, at the film/substrate interface.

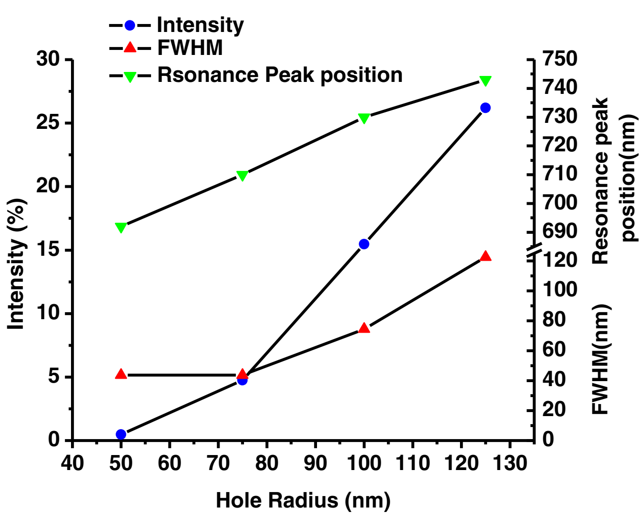

Fig. 3 The effects of varying of hole radius on the transmission peak intensity, FWHM, and resonance peak position of the film/substrate, $\lambda_{(1,\ 0)}$, in a nano-hole array-perforated gold film supported by silica and hole depth of 100 and structural period of 400 nm

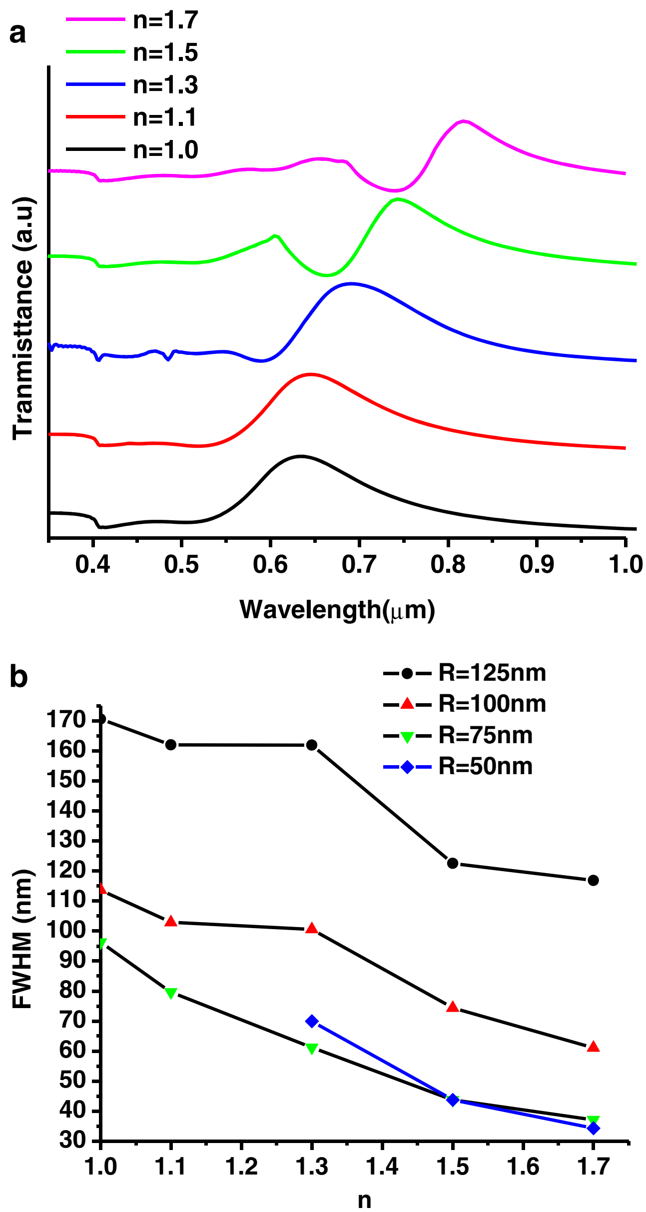

Fig. 4 The effects of varying of substrate refractive index on **a** optical transmission spectra at hole radius of 125 nm and **b** on the FWHM of the first surface plasmon resonance order at different hole radius of the nano-hole array of hole depth of 100 nm and structural period of 400 nm

As it is clear from this figure, the surface plasmon resonance peak at the air/film (cladding layer/film) interface performs a significant contribution to the transmittance spectra at wavelength of $\lambda_{(1,\ 0)}$=604 and 664 nm for refractive indices of 1.5 and 1.7, respectively.

The effects of using a supporting medium with different refractive indices in the range of 1 to 1.7 on the FWHM values of the $\lambda_{(1,\ 0)}$ of SPR of the NHA at different hole radiuses in the range of 50 to 125 nm are compared in Fig. 4b. As can be seen from this figure, the SPR transmission footprint was observed on using supported layer of refractive index of 1.3 in a structure of hole radius of 50 nm, while on using the larger hole radius, the SPR footprint was acquired at a lower index than 1.3.

From this figure, it is clear that the FWHM values of the $\lambda_{(1,\ 0)}$ of the SPR in a NHA of fix hole radius were decreased on increasing the refractive index from 1 to 1.7. The minim FWHM for all hole radiuses occurred when the NHA was perforated on the substrate with a refractive index of 1.7.

It is also clear that the FWHM value of NHAs was higher at a lower substrate refractive index and larger hole radius. It can be seen that, on increasing the substrate index form 1.0 to 1.7, the FWHM values were reduced by 36, 55, 53, and 54 nm for the NHA with hole radius of 50, 75, 100, and 125 nm, respectively. The maximum FWHM values were observed at free-standing film NHA (i.e., n=1) as 96 nm for hole radius of 75 nm and were increased to 171 nm at hole radius of 125 nm, while the minimum of 34 nm was observed in a hole radius of 50 nm and increased to 117 nm at hole radius of 125 nm.

The effects of varying of substrate refractive index on the $\lambda_{(1,\ 0)}$ resonance wavelength position in the NHA at different hole radiuses are compared in Fig. 5a. As can be seen from this figure, on increasing the substrate refractive index, the resonance wavelength position was linearly increased by 210, 204, 191, and 185 nm in the NHA of hole radius of 50, 75, 100, and 125 nm, respectively.

It was also found that the maximum variation of the resonance wavelength position at film/substrate interface due to increasing the hole radius from 50 to 125 nm was obtained as 78 nm in perforated structure on the substrate with refractive index of 1.7. While the minimum one was acquired as 49 nm.

Figure 5b shows the effects of the substrate refractive index variation on the resonance intensity, in the NHA. As can be seen from this figure, the maximum resonance intensity was obtained on using a substrate with refractive index of 1.3 and minimum one was acquired on using the substrate index of 1.7.

This could be due to lower energy matching between the localized electric filed at the both interfaces of the nano-hole structure on increasing the refractive index differences between two interfaces [25]. The energy mismatching between

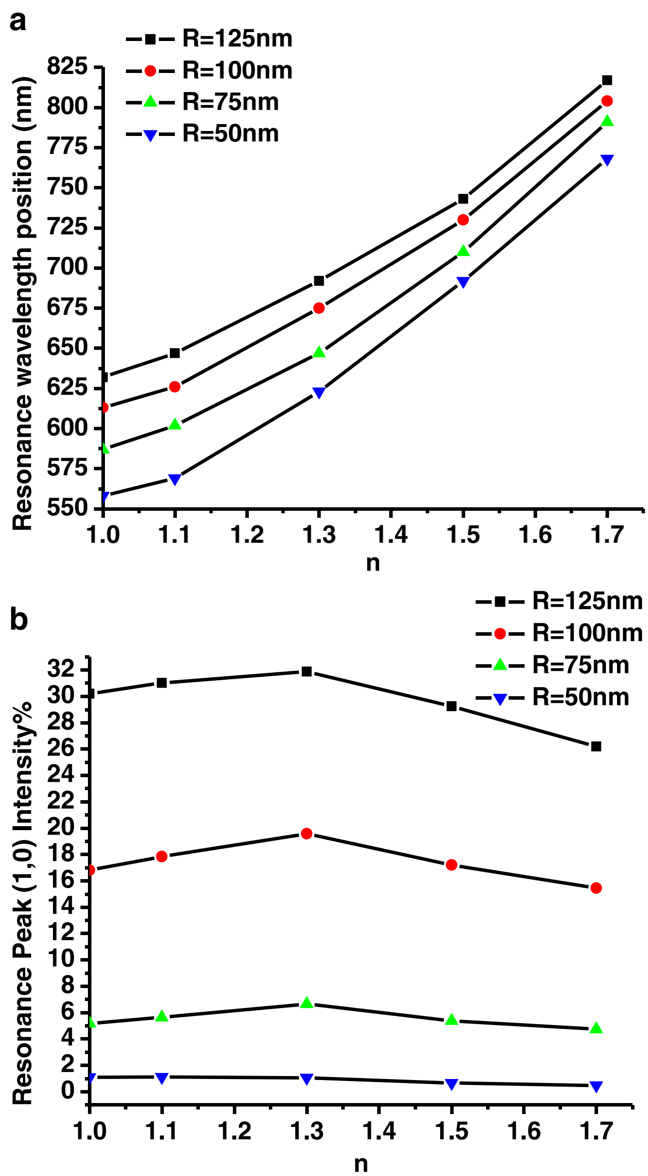

Fig. 5 The effects of varying of the substrate refractive index on the **a** resonance wavelength and **b** resonance intensity of the first transmission diffraction order at the film/substrate interface in the nano-hole array at different hole radiuses, hole depth of 100 nm, and structural period of 400 nm

both interfaces becomes more significant on using larger hole radius in the NHA as is evident in Fig. 5b. It is also clear that the transmission intensity of the $\lambda_{(1,\ 0)}$ SP mode was increased on increasing the refractive index from 1 to 1.3 and then reduced to its minimum value on increasing the substrate index of refraction to 1.7.

The effects of variation of substrate index of refraction on the optical transmission intensity of the nano-hole structure were reported in Table 2. As can be seen from this table, it is clear that on increasing the refractive index of the supported layer, the transmission intensity of the resonance wavelength

Table 2 The effects of variation of the refractive index of the ambient layer on the resonance transmission intensity (T%) in a nano-hole array structure at different hole radius, hole depth of 100 nm, and period of 400 nm

Hole_r (nm)	n					Δ_n% ↓
	1.0	1.1	1.3	1.5	1.7	
125	30.2	31.0	31.9	29.2	26.2	4
100	16.8	17.8	19.6	17.2	15.5	1.3
75	5.2	5.6	6.7	5.4	4.7	0.5
50	1.1	1.1	1.0	0.6	0.5	0.6

was decreased. The maximum reduction was observed as 4 % in the structure of hole radius of 125, while the minimum one was obtained as 0.5 % on using the hole radius of 75 nm.

The sensitivity of a NHA depends on the dielectric constant of the medium and the geometrical parameters of the NHA. The sensitivity, S, at normal incidence is given by [27]:

$$S = \frac{\Delta \lambda}{\Delta n} = \frac{P}{\sqrt{i^2 + j^2}} \sqrt{\left(\frac{\varepsilon_m}{\varepsilon_d + \varepsilon_m}\right)^3} \tag{3}$$

where S is the sensitivity, $\Delta\lambda$ is the resonance wavelength shift due to refractive index change, Δn, P is the structural period, i and j are integer numbers corresponding to the SPR mode, and ε_m and ε_d are the relative permittivity of the metal and dielectric. As can be seen from Eq. 3, the sensitivity of the NHA is strongly dependent on the structural periodicity of the NHA, the transmission diffraction order, and the relative permittivity of the metal and the dielectric material around the NHA as well as the resonance wavelength shift. Since the sensitivity is inversely proportional to transmission order, the lowest order transmission mode would be most sensitive to the refractive index variation. The sensitivity of the NHA is also affected by variation of the hole radius. Table 3 compares the sensitivity of the NHA due to variation of the hole radius which yields to the spectral wavelength shift and refractive index variation in a NHA.

Table 3 Spectral sensitivity, S_r, and index sensitivity, S_n, of the NHA at different hole radius. S_r values were calculated relative to the free-standing film NHA (n=1.0)

Hole_r (nm)	S_r (nm/RIU)				n	S_n (nm/RIU)
	1.1	1.3	1.5	1.7	1.0	454
125	150	200	222	264	1.1	460
100	130	207	234	273	1.3	473
75	150	200	246	291	1.5	485
50	110	217	268	300	1.7	499

The effects of varying of the refractive index of the substrate on the sensitivity, S_n, were increased from 454 to 499 nm/RIU on increasing the refractive index from 1 to 1.7, although it was found that for a larger index of refraction (e.g., 1.5 and 1.7) on increasing the hole radius, the spectral sensitivity, S_r, due to the spectral wavelength shift of the $\lambda_{(1,\ 0)}$ was decreased. The maximum spectral sensitivity was acquired as 300 nm/RIU in the NHA of hole radius of 50 nm and substrate index of 1.7, whereas the minimum one was 110 nm/RIU at hole radius of 50 nm and supported layer index of 1.1. However, by using the SP resonance dispersion equation, the maximum sensitivity of the NHA due to refractive index changes was calculated as 499 nm/RIU at the index of 1.7.

The difference between the S_r and S_n could be attributed to the spectral wavelength shift in the NHA due to the variation of the hole radius, which does not consider in the SP dispersion relation. It is clear that, on increasing the hole radius, more light passes through the nano-hole, and therefore, this could affect the coupling properties between SPR evanescent wave and light through the nano-hole.

In conclusion, the effects of the varying of hole radius and the supported layer index of refraction on the optical transmittance properties of the perforated NHA on the supported gold film of thickness of 100 nm were numerically studied. It was found that transmission properties (i.e., FWHM, SP resonance position, and intensity) were strongly affected by hole radius and the substrate index variation in an array of fix hole depth and structural periodicity. In the small hole radiuses (<50 nm), the bulk plasmon frequency was observed as the dominant transmission peak at wavelength of 470 to 500 nm [25], while on increasing the hole radius, the surface plasmon resonance becomes more dominant than the bulk plasmon frequency of the gold film as it was shown in Fig. 2a.

The maximum transmission intensity of the $\lambda_{(1,\ 0)}$ was calculated as 31.9 % in a NHA structure of hole radius of 125 nm and substrate refractive index of 1.3, whereas the minimum one was acquired as 0.5 % at hole radius of 50 nm and substrate refractive index of 1.7 as reported in Table 2.

It was also observed that, on increasing the hole radius of the NHAs, the resonance wavelength was shifted towards longer wavelength, which is in agreement with the pervious works [5] and confirms the validity of this study. The SP wavelength was shifted towards longer wavelength on increasing the refractive index by 185 nm. This wide range of redshift could be promising high potential of the refractive index sensing application, which can be tuned by changing the hole radius of the NHA structure.

It was also reported that, on increasing the substrate index of refraction, the FWHM values were decreased; however, they were increased on increasing the hole radius of the NHA. Therefore, using the substrate of high index of refraction and smaller hole radius in the perforated structure could increase the sensitivity of the NHA structure.

The spectral sensitivity of 300 nm/RIU was obtained for a NHA of hole radius of 50 nm and substrate index of refraction of 1.7. It was also shown that the index sensitivity due to the SP dispersion relation increased from 454 to 499 nm/RIU on increasing the refractive index from 1.0 to 1.7.

References

1. Ebbesen TW, Lezec HJ, Ghaemi HF, Thio T, Wolff PA (1998) Extraordinary optical transmission through sub-wavelength hole arrays. Nature 391(6668):667–669
2. Bethe HA (1944) Theory of diffraction by small holes. Phys Rev 66(7–8):163–182
3. Li J-Y, Hua Y-L, Fu J-X, Li Z-Y (2010) Influence of hole geometry and lattice constant on extraordinary optical transmission through subwavelength hole arrays in metal films. J Appl Phys 107(7):073101–073108
4. Correia-Ledo D, Gibson KF, Dhawan A, Couture M, Vo-Dinh T, Graham D, Masson J-F (2012) Assessing the location of surface plasmons over nanotriangle and nanohole arrays of different size and periodicity. J Phys Chem C 116(12):6884–6892. doi:10.1021/jp3009018
5. Wu L, Bai P, Li EP (2012) Designing surface plasmon resonance of subwavelength hole arrays by studying absorption. J Opt Soc Am B 29(4):521–528
6. Barnes WL, Dereux A, Ebbesen TW (2003) Surface plasmon subwavelength optics. Nature 424(6950):824–830
7. Maier SA (2007) Plasmonic: fundamentals and applications. Springer, Heidelberg
8. Hajiaboli AR, Cui B, Kahrizi M, Truong V-V (2009) Optical properties of thick metal nanohole arrays fabricated by electron-beam and nanosphere lithography. Phys Status Solidi (A) 206(5):976–979. doi:10.1002/pssa.200881294
9. Brolo AG, Gordon R, Leathem B, Kavanagh KL (2004) Surface plasmon sensor based on the enhanced light transmission through arrays of nanoholes in gold films. Langmuir 20(12):4813–4815. doi:10.1021/la0493621
10. Xiao S, Mortensen NA, Qiu M (2007) Enhanced transmission through arrays of subwavelength holes in gold films coated by a finite dielectric layer. J Europ Opt Soc Rap Public 2:07009
11. Huang H, Liu X, Liao B, Chu P (2011) A localized surface plasmon resonance biosensor based on integrated controllable Au_2S/AuAgS-coated gold nanorods composite. Plasmonics 6(1):1–9. doi:10.1007/s11468-010-9162-7
12. Xia L, Yin S, Gao H, Deng Q, Du C (2011) Sensitivity enhancement for surface plasmon resonance imaging biosensor by utilizing gold–silver bimetallic film configuration. Plasmonics 6(2):245–250. doi:10.1007/s11468-010-9195-y
13. Genet C, Ebbesen TW (2007) Light in tiny holes. Nature 445(7123):39–46
14. Coe JV, Williams SM, Rodriguez KR, Teeters-Kennedy S, Sudnitsyn A, Hrovat F (2006) Extraordinary IR transmission with metallic arrays of subwavelength holes. Anal Chem 78(5):1384–1390. doi:10.1021/ac069371
15. Alkaisi MM, Blaikie RJ, McNab SJ, Cheung R, Cumming DRS (1999) Sub-diffraction-limited patterning using evanescent near-field optical lithography. Appl Phys Lett 75(22):3560–3562
16. Luo X, Ishihara T (2004) Subwavelength photolithography based on surface-plasmon polariton resonance. Opt Express 12(14):3055–3065
17. Liu Y, Blair S (2003) Fluorescence enhancement from an array of subwavelength metal apertures. Opt Lett 28(7):507–509
18. Garrett SH, Smith LH, Barnes WL (2005) Fluorescence in the presence of metallic hole arrays. J Mod Opt 52(8):1105–1122. doi:10.1080/09500340512331323457
19. Battula A, Chen S, Lu Y, Knize RJ, Reinhardt K (2007) Tuning the extraordinary optical transmission through subwavelength hole array by applying a magnetic field. Opt Lett 32(18):2692–2694
20. Gao H, McMahon JM, Lee MH, Henzie J, Gray SK, Schatz GC, Odom TW (2009) Rayleigh anomaly-surface plasmon polariton resonances in palladium and gold subwavelength hole arrays. Opt Express 17(4):2334–2340
21. Chang S-H, Gray S, Schatz G (2005) Surface plasmon generation and light transmission by isolated nanoholes and arrays of nanoholes in thin metal films. Opt Express 13(8):3150–3165
22. Alexandre V, Thierry L (2007) Description of dispersion properties of metals by means of the critical points model and application to the study of resonant structures using the FDTD method. J Phys D: Appl Phys 40(22):7152
23. Rakic AD, Djurisic AB, Elazar JM, Majewski ML (1998) Optical properties of metallic films for vertical-cavity optoelectronic devices. Appl Opt 37(22):5271–5283
24. Ghaemi HF, Thio T, Grupp DE, Ebbesen TW, Lezec HJ (1998) Surface plasmons enhance optical transmission through subwavelength holes. Phys Rev B 58(11):6779–6782
25. Najiminaini M, Vasefi F, Kaminska B, Carson JJL (2012) Effect of surface plasmon energy matching on the sensing capability of metallic nano-hole arrays. Appl Phys Lett 100(6):063110–063114
26. Laux E, Genet C, Ebbesen TW (2009) Enhanced optical transmission at the cutoff transition. Opt Express 17(9):6920–6930
27. Pang L, Hwang GM, Slutsky B, Fainman Y (2007) Spectral sensitivity of two-dimensional nanohole array surface plasmon polariton resonance sensor. Appl Phys Lett 91(12):123112–123113